



# A new marine biogenic emission: methane sulfonamide (MSAM), DMS and DMSO<sub>2</sub> measured in air over the Arabian Sea

Achim Edtbauer<sup>1</sup>, Christof Stöner<sup>1</sup>, Eva Y. Pfannerstill<sup>1</sup>, Matias Berasategui<sup>1</sup>, David Walter<sup>1,2</sup>, John N. Crowley<sup>1</sup>, Jos Lelieveld<sup>1,3</sup>, and Jonathan Williams<sup>1,3</sup>

<sup>1</sup>Atmospheric Chemistry Department, Max Planck Institute for Chemistry, Mainz, Germany

<sup>2</sup>Department Biogeochemical Processes, Max Planck Institute for Biogeochemistry, Jena, Germany

<sup>3</sup>Energy, Environment and Water Research Center, The Cyprus Institute, Nicosia, Cyprus

**Correspondence:** Achim Edtbauer (a.edtbauer@mpic.de)

**Abstract.** We present the first ambient measurements of a new marine emission methane sulfonamide (MSAM) along with dimethyl sulfide (DMS) and dimethyl sulfone (DMSO<sub>2</sub>) over the Arabian Sea. Two shipborne transects (W → E, E → W) were made during the AQABA (Air Quality and Climate Change in the Arabian Basin) measurement campaign. DMS mixing ratios were in the range 0.3–0.5 ppb during the first traverse of the Arabian Sea (first leg) and 0.1 to 0.3 ppb in the second leg. In the first leg DMSO<sub>2</sub> was always below 0.04 ppb and MSAM was close to the limit of detection. During the second leg DMSO<sub>2</sub> was between 0.04–0.12 ppb and MSAM was mostly in the range 0.02–0.05 ppb with maximum values of 0.06 ppb. An analysis of HYSPLIT back trajectories combined with calculations of the exposure of these trajectories to *chlorophyll a* content in the water revealed that most MSAM originates from the Somalia upwelling region, known for its high biological activity. This new marine emission is of particular interest as it contains both sulfur and nitrogen, making it potentially relevant to marine nutrient cycling and particle formation.

## 1 Introduction

~~Sulfur and nitrogen are essential for all lifeforms and the ocean plays an important role in the global cycling of both elements. The ocean represents a large reservoir for sulfur, some of which can enter the atmosphere in organically bound forms such as dimethyl sulfide (DMS).~~ DMS emitted from the oceans accounts for roughly half of the natural global atmospheric sulfate burden. A recent estimate of global DMS flux to the atmosphere is 28.1 (17.6–34.4) Tg S per year which amounts to around 50 % of the anthropogenic sulfur inputs (Webb et al., 2019). ~~In contrast,~~ nitrogen is usually a limiting nutrient for phytoplankton growth (Voss et al., 2012) with nitrate deposition from the air and oceanic upwelling being important factors in the oceans primary productivity.

Upwelling regions in the oceans are those where nutrient rich waters from depths of 100 to 300 meters are brought to the surface (Voss et al., 2013; Kämpf and Chapman, 2016) and in which highly specialized marine organisms can proliferate. In the Arabian Sea, the location of this study, the Somali coastal upwelling is a major feature. It is considered the fifth largest upwelling system in the world (deCastro et al., 2016; Ajith Joseph et al., 2019). Upwelling generally leads to eutrophic zones in the surface ocean and therefore to regions of high phytoplankton activity, resulting in high carbon dioxide uptake and the



release of various volatile organic compounds including sulfur, halogen and alkene containing trace gases (Arnold et al., 2010; Colomb et al., 2008; Bonsang et al., 2010; Lai et al., 2011; Yassaa et al., 2008). These species can impact ozone formation and loss in the marine boundary layer (e.g. Williams et al. (2010)).

In the oceans, biochemical reactions within phytoplankton result in the production of dimethylsulphoniopropionate (DMSP), the primary biological precursor for DMS in the ocean (Kiene et al., 2000). A small fraction of the DMS produced in the ocean is released into the atmosphere (Vila-Costa et al., 2006), where it is oxidized predominantly by the hydroxyl radical (OH), ultimately yielding sulfates which may act as cloud condensation nuclei (see Fig. 1). Even though only a small fraction of DMS is released to the atmosphere, it is still the most abundant form in which the ocean releases gaseous sulfur (Kloster et al., 2006; Quinn and Bates, 2011; Lana et al., 2011; Liss et al., 2014). This makes DMS an important component of the global sulfur cycle (Bentley and Chasteen, 2004; Barnes et al., 2006; Zavarisky et al., 2011). The oxidation mechanisms of DMS in the atmosphere are complex and still not fully understood (Mardyukov and Schreiner, 2018; Barnes et al., 2006; Ayers and Gillett, 2000; Chen et al., 2018). DMSO<sub>2</sub> can be formed from OH oxidation of DMS directly, via the intermediate dimethyl sulfoxide (DMSO) and from oxidation of DMSO with BrO and NO<sub>3</sub> (Barnes et al., 2006).

Marine emissions containing reactive nitrogen are generally found at much lower mixing ratios than sulfur. Nitrogen is a limiting nutrient to pelagic ecosystems. Alkyl nitrates (RONO<sub>2</sub>) have been observed in equatorial upwelling areas at low ppt levels (Chuck et al., 2002) and methylated amines were also present at similarly low concentrations (Ge et al., 2011). To date, no compound containing both sulfur and nitrogen has been identified as a marine emission.

In this study we present trace gas measurements taken on a shipborne circumnavigation of the Arabian Peninsula. Relatively few measurements have been made in this region due to political tensions and piracy. Transects of the Arabian Sea (the most southerly section of the route) showed high levels of sulfur containing gases. These include DMS, DMSO<sub>2</sub> and a new sulfur containing species, methane sulfonyl fluoride (MSF). The provenance of these species is investigated with respect to chlorophyll exposure of the airmasses sampled.

## 2 Materials and Methods

### 2.1 AQABA campaign

From June 25th to September 3rd 2017, the Air Quality and Climate Change in the Arabian Basin (AQABA) cruise took place on the research vessel *Kommandor Iona*. The first leg of the cruise started from La-Seyne-sur-mer near Toulon (France), and headed through the Suez Canal, around the Arabian Peninsula and ended in Kuwait. The second leg took the same route back (see Fig. 2). Onboard the ship were a weather station and four laboratory containers equipped with instrumentation for on- and offline measurement of a large suite of trace gases, particles and radicals (Bourtsoukidis et al., 2019).

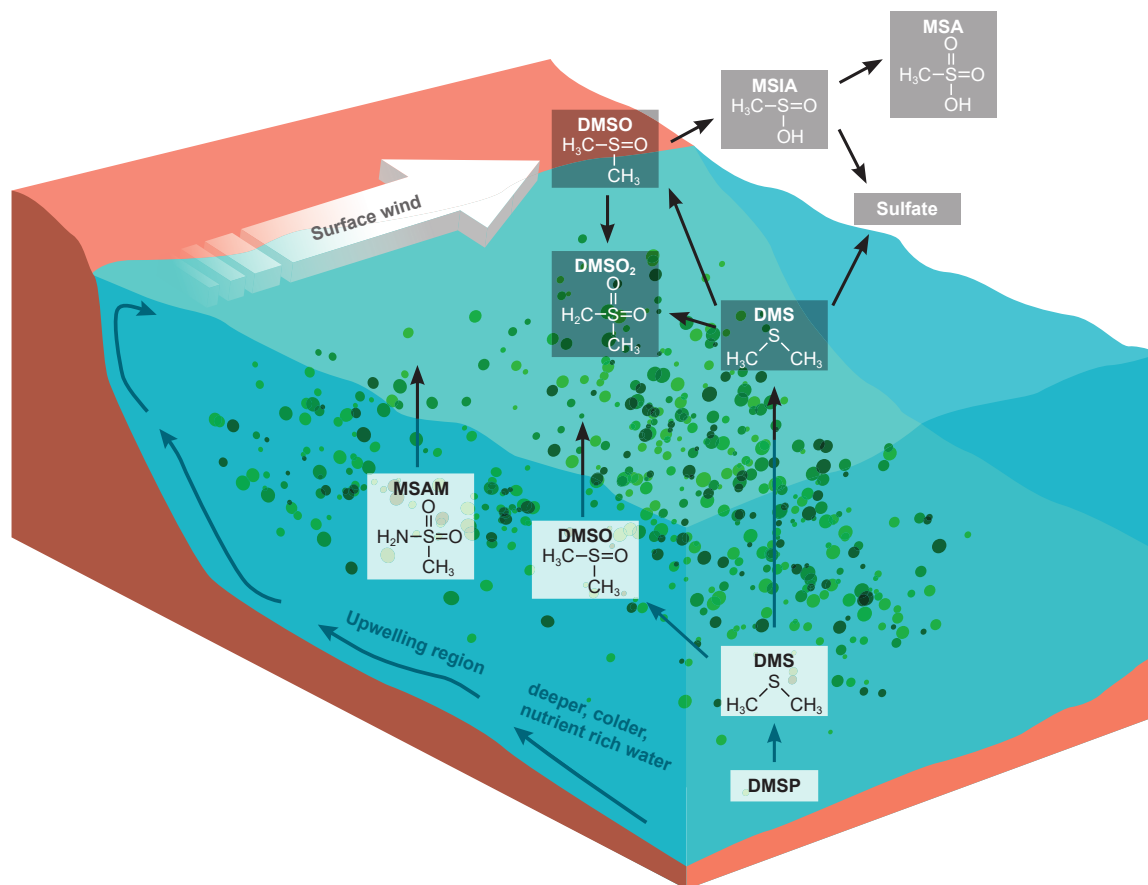


**Figure 1.** DMS oxidation scheme focusing on the trace gases discussed by Jarnes et al., 2006). The bottom part of the figure illustrates the principle of the Somalia upwelling. Wind blowing along the coast displaces surface water and leads to upwelling of cold nutrient rich water which can support a phytoplankton bloom (Kämpf and Chapman, 2016).

## 2.2 Sampling

A 5.5 m high (above deck level) high volume-flow inlet (HUF) (diameter 15 cm) was used to draw ambient air down to the containers at a flow rate of 10 m<sup>3</sup>/min. The HUF was situated between the four containers on the foredeck so that when the ship headed into the wind no interference from the vessel's smokestack or indoor ventilation were measured. From the center of the HUF, air was drawn continuously at a rate of ca. 5 standard liter per minute (slpm) (first leg) or 3 slpm (second leg) into an air-conditioned laboratory container via an insulated FEP (fluorinated ethylene propylene) tube (1/2" = 1.27 cm i.d., length ca. 10 m). The tube was heated to 50–60 °C to avoid condensation inside the air-conditioned container. To prevent sampling of sea spray and particles, a weekly changed PTFE (polytetrafluoroethylene) filter was installed in the inlet line before it entered the container. This inlet system was employed for the measurements of VOCs and total OH reactivity (Pfannerstill et al., 2019)

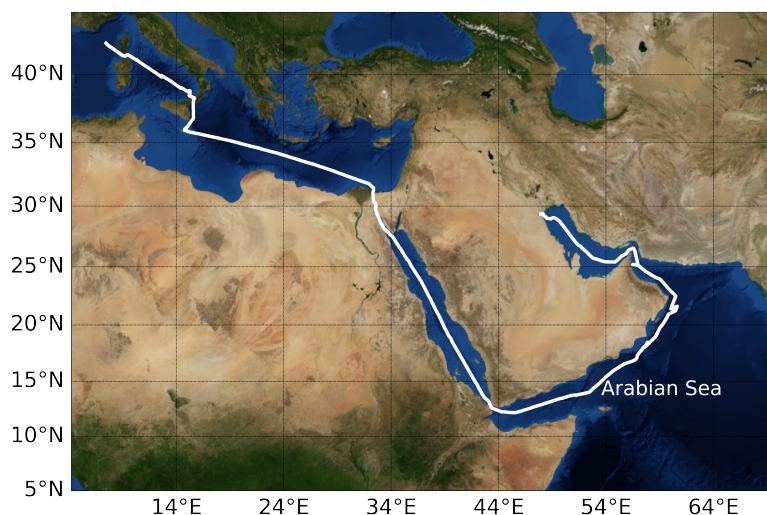


**Figure 2.** Ship track of AQABA cruise. Beginning of July 2017 the campaign started in the south of France near Toulon, the ship arrived in Kuwait at the end of July, started its return back to France beginning of August and was back at its starting point beginning of September 2017. On the way towards Kuwait it entered the Arabian Sea on the 19<sup>th</sup> of July and left it on the 24<sup>th</sup> of July. On the way back it entered the Arabian Sea on the 11<sup>th</sup> of August and left it on the 15<sup>th</sup> of August. Credit: NASA Earth Observatory.

simultaneously. The inlet residence time for the VOC measurements was determined by a spiking test with acetone, and was 12 s during the first leg and 26 s during the second leg.

### 2.3 Volatile Organic Compounds (VOCs) measurements

Online volatile organic compounds (VOCs) measurements were performed using a proton transfer reaction time-of-flight mass spectrometer (PTR-TOF-MS 8000, Manufacturer: Ionicon Analytik GmbH, Innsbruck, Austria). Detailed descriptions of the instrument can be found in Jordan et al. (2009); Graus et al. (2010); Veres et al. (2013). Proton transfer is a soft ionization technique resulting in little fragmentation which simplifies molecular identification. Drift pressure was maintained at 2.2 mbar and the drift voltage at 600 V (E/N 137 Td). For mass scale calibrations, 1,3,5-trichlorobenzene was continuously fed into the sample stream. The PTR-TOF-MS was calibrated at the beginning, during and at the end of the campaign (in total five humidity dependent calibrations were conducted as described by Derstroff et al. (2017)). Calibrations were performed by using a standard gas mixture (Apel-Riemer Environmental inc., Broomfield, USA) of several VOCs with known, gravimetrically determined mixing ratios. The VOCs included in the calibration gas were: methanol, acetonitrile, acetaldehyde, acetone, dimethyl sulfide, isoprene, methyl vinyl ketone, methacrolein, methyl ethyl ketone, benzene, toluene, o-xylene, 1,3,5-trimethylbenzene and  $\alpha$ -





pinene. Clean synthetic air was measured every three hours for ten minutes to determine the instrument background. The time resolution of the measurement was 1 minute and the mass range extended to 450 amu. Mass resolution (full width half maximum) was ca. 3500 during the first leg and > 4500 during the second leg at mass 96 amu.

The total uncertainty of the DMS measurement was < 30% (main sources of uncertainty: standard gas mixture 5%, flow meter 1%, calibration  $\approx$  10%), and the precision < 5 %. DMSO<sub>2</sub> and MSAM were not present in the calibration gas. Calculation of the mixing ratio was therefore conducted based on theory and more specifically the rate coefficients for proton transfer (Su and Chesnavich, 1982; Chesnavich et al., 1980), the knowledge of transmission factors, amount of H<sub>3</sub>O<sup>+</sup> ions and parameters of the drift region (Lindinger et al., 1998). Applying this method results in a greater uncertainty than for compounds included in the calibration gas mixture of approximately 50% due to the fact that we do not know the inlet transmission for these two substances, we conservatively estimate an uncertainty of up to a factor of 2 for MSAM and DMSO<sub>2</sub>.

## 2.4 HYSPLIT back trajectories

Air mass back trajectories were calculated to investigate the origin of air masses encountered. The Hybrid Single-Particle Lagrangian Integrated Trajectory model (HYSPLIT, version 4, 2014), a hybrid between a Lagrangian and an Eulerian model for tracing small imaginary air parcels forward or back in time (Draxler and Hess, 1998), was used to derive back trajectories from a starting height of 200 m above sea level, going 216 hours back in time on an hourly grid beginning at the ship position.

## 3 Results

### 3.1 Dimethyl sulfide (DMS)





Measurements of DMS (m/z 63.0263) during AQABA showed elevated mixing ratios when the vessel traversed the Arabian Sea during both legs (brown shaded region in Fig. 3 a). During the first leg over the Arabian Sea (Fig. 3 b), DMS mixing ratios were generally in the range of 0.3–0.5 ppbv, with occasional peaks of 0.8 ppbv. During the second leg (Fig. 3 c), the DMS mixing ratios over the Arabian Sea were significantly lower in the range of 0.1–0.3 ppbv, again with elevated peaks of short duration (around 2 h).

### 3.2 Dimethyl sulfone (DMSO<sub>2</sub>)

Dimethyl sulfone (DMSO<sub>2</sub>) is an oxidation product of DMS by the OH radical (Arsene et al., 2001; Barnes et al., 2006). It was measured by the PTR-ToF-MS at m/z 95.0161. A thorough investigation of other plausible mass formulas, which would yield a m/z value inside the error margins due to the mass resolution, gave no plausible alternative molecular structure. Additionally, the head space of the pure compound (TCI Deutschland GmbH, purity > 99 %) was sampled yielding a peak at the same position as found in ambient air. Therefore we assigned this mass to DMSO<sub>2</sub>. Measurements of DMSO<sub>2</sub> in the Arabian Sea region showed elevated levels between 0.04–0.12 ppb during the second leg (Fig. 3 c)) but more modest levels (< 0.04 ppb) in leg 1 (Fig. 3 b)). To our knowledge, there have been no measurements of DMSO<sub>2</sub> performed in this region previously.




### 3.3 New atmospheric trace gas: Methane sulfonamide (MSAM)

At  $m/z$  96.0144, a signal was observed which displayed a strong correlation with  $\text{DMSO}_2$  (Pearson correlation coefficient:  $r$  around 0.8) over the Arabian sea during the second leg (see Fig. 4). This mass corresponded to methane sulfonamide (MSAM), which has a similar structure to  $\text{DMSO}_2$   difference being that one methyl group is replaced by an amine group (see Fig. 1 for the chemical structures of the molecules). This molecule has not previously been measured in ambient air. To confirm the assignment of mass  $m/z$  96.0144 to MSAM, the head-space of the pure substance MSAM (Alfa Aesar, purity > 98 %) was sampled by the PTR-ToF-MS. The analysis of the pure compound MSAM by PTR-ToF-MS matched the mass found in ambient air. No other plausible molecular structures could be found for this mass within the error margins due to the mass resolution  Based on the correlation of mass  $m/z$  96.0144 to  $\text{DMSO}_2$  in ambient data, the mass spectral match to the pure compound, and the absence of alternative structures at that exact mass we identify the measured signal as MSAM. In order to test whether MSAM can be observed outgassing from seawater, we flushed the headspace of solutions of  $4.2 \text{ mol L}^{-1}$ ,  $0.05 \text{ mol L}^{-1}$  and  $0.0005 \text{ mol L}^{-1}$  MSAM in artificial seawater with  $100$ ,  $50$  and  $25 \text{ ml min}^{-1}$  of synthetic air (Air Liquide, Krefeld, Germany) each. The resulting mixing ratios measured ranged from  $0.65 \text{ ppb}$  (lowest concentration and lowest flow rate) to  $130 \text{ ppb}$  (highest concentration and highest flow rate)  During the Arabian Sea section of the second leg, values of up to  $0.06 \text{ ppb}$  were measured, but mostly it was found in the range of  $0.02$ – $0.05 \text{ ppb}$ . In the first leg, MSAM was occasionally detected in the Arabian Sea, but concentrations were generally close to the limit of detection (LOD)  which was  $5 \text{ ppt}$  ( $3 \times$  standard deviation of background).

## 4 Discussion

Here we discuss DMS,  $\text{DMSO}_2$  and MSAM measurements in air from a rarely sampled region, the Arabian Sea. First we discuss the difference in DMS abundance between the two legs. Secondly we evaluate the source regions of these trace gases based on knowledge of their atmospheric lifetimes and chlorophyll exposure. Then finally we address the implications of these measurements to marine boundary layer chemistry.

### 4.1 DMS

 surface DMS concentrations can be used to estimate DMS fluxes to the atmosphere and a global climatology of DMS flux values has been derived by Lana et al. (2011) from over 47000 seawater measurements worldwide. Lana et al. predict strong fluxes of DMS in the Arabian Sea region, particularly in June, July and August, coincident with the AQABA campaign. Seawater concentration data for DMS from the Lana climatology relevant for AQABA has been plotted in Fig. 5 for July and August. In the regions south of the Arabian Peninsula, higher concentrations of DMS in seawater are expected in July than in August. The observed higher measured values of DMS seen on the AQABA first leg are consistent with this. The highest DMS mixing ratios occurred during the first leg over the Gulf of Aden with around  $0.8 \text{ ppb}$ . The peak values are likely related to the ship crossing directly through patches of phytoplankton as evidenced by the observation of strong bioluminescence around the

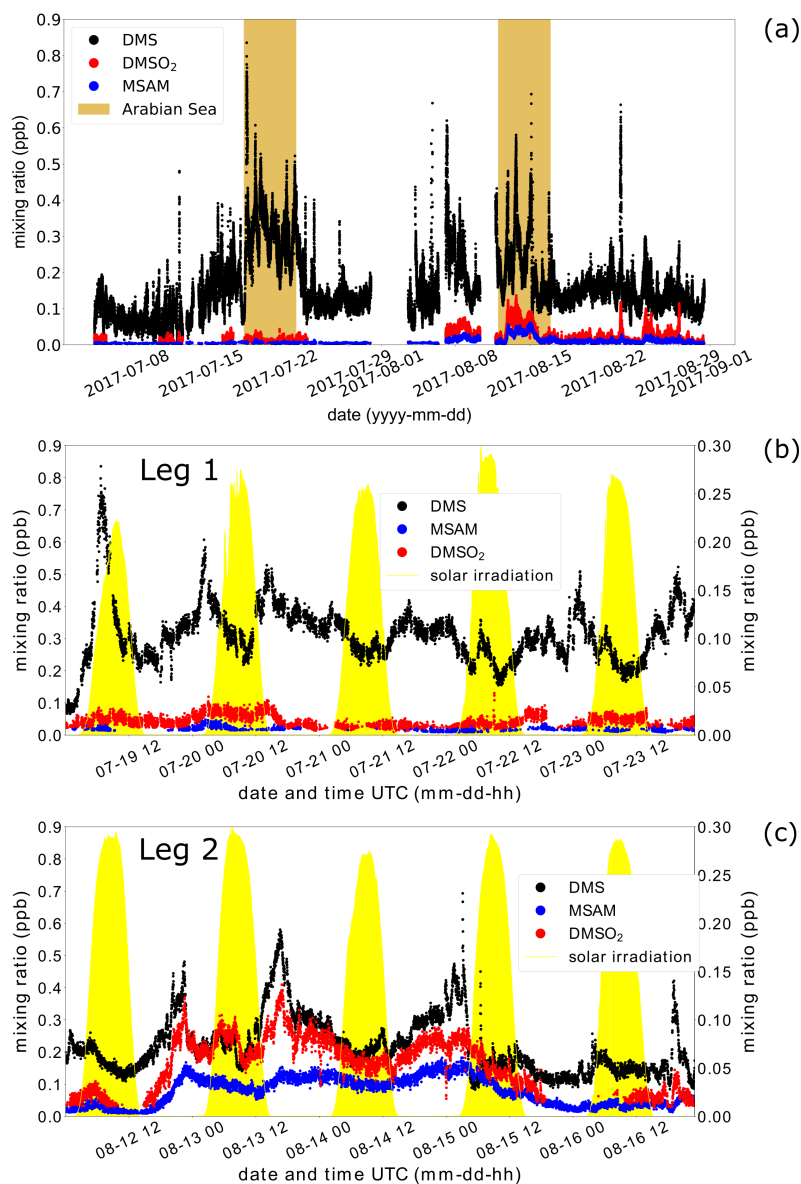


**Figure 3.** In panel (a) the mixing ratios of for DMS, DMSO<sub>2</sub> and MSAM during the whole AQABA cruise are displayed. The Arabian Sea parts of leg 1 and 2 are marked with brown. A zoom-in on measurements over the Arabian Sea is given for leg 1 in panel (b) and for leg 2 in panel (c). The y-axis for MSAM and DMSO<sub>2</sub> (panels (b,c)) is on the right (DMS on the left) and the yellow filled curves in panels (b,c) show the solar irradiation in arbitrary units.

ship during the night. The DMS mixing ratio values of up to 0.3 ppb during the second leg can be compared to measurements made previously in that region during a cruise on the research vessel Pelagia in April 2000, DMS values up to 0.25 ppb

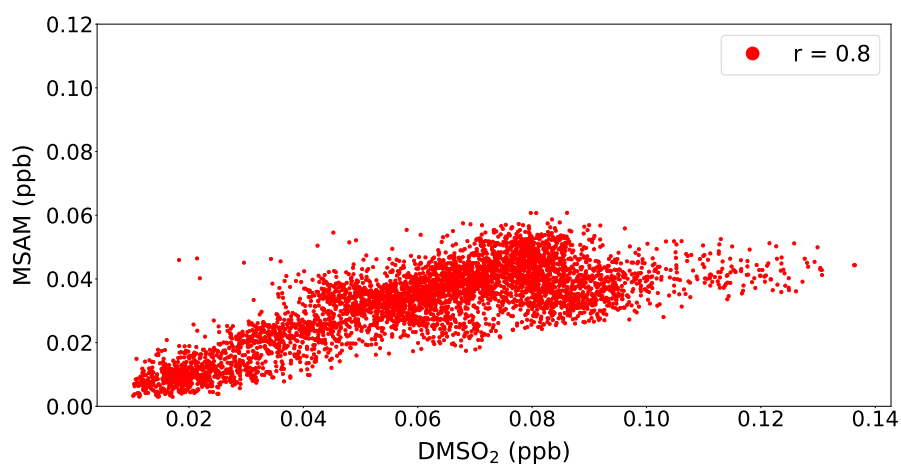


**Figure 4.** Correlation of MSAM with DMSO<sub>2</sub> during the second leg in the Arabian Sea.

associated with upwelling in the Gulf of Aden were reported (Warneke and de Gouw, 2001). More recent measurements during a ship cruise in July and August 2018 in the western tropical Indian Ocean reported values of up to 0.3 ppb DMS (Zavarsky et al., 2018). The DMS measurements presented here are therefore consistent with the very limited previous measurements in this region.

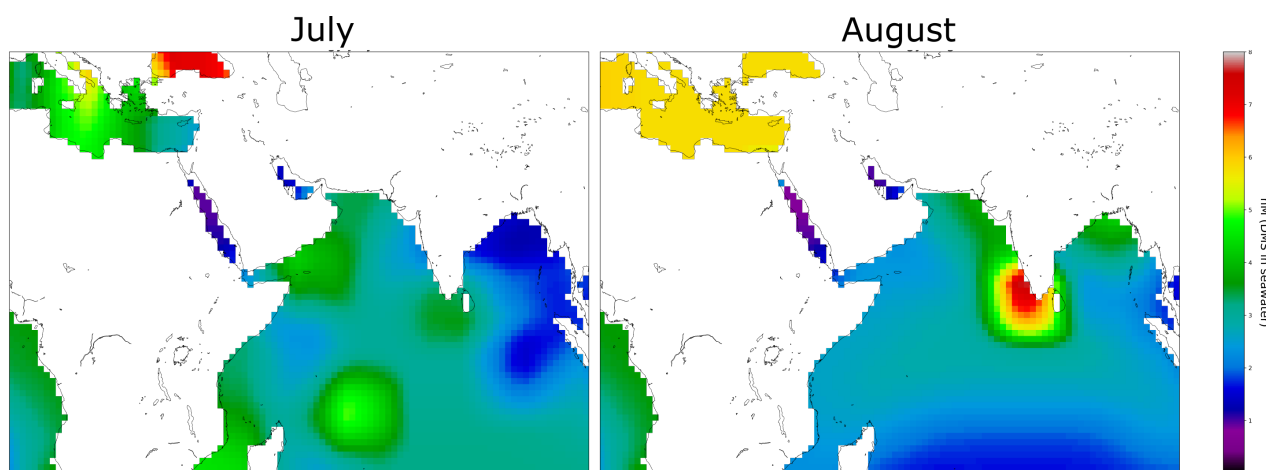


**Figure 5.** Climatology for DMS sea surface water concentrations in July and August (Lana et al., 2011).



## 4.2 Atmospheric lifetimes of DMS, DMSO<sub>2</sub> and MSAM

The lifetime of DMS in the atmosphere with respect to the primary oxidant OH is around 1.3 days (reaction rate =  $7.8 \times 10^{-12} \text{ cm}^3 \text{ molec}^{-1} \text{ s}^{-1}$ , [OH] =  $1.1 \times 10^6 \text{ molec/cm}^3$  (Ito et al., 2006)). In some regions of the marine boundary layer, BrO may also contribute to the oxidation of DMS leading to shorter DMS lifetimes (Breider et al., 2010; Khan et al., 2016; Barnes et al., 2006). The high and variable levels of DMS encountered during the Arabian Sea crossing suggest that DMS mixing ratios are influenced by local variation of the sources (i.e. phytoplankton patches). The reaction rate of OH and DMSO<sub>2</sub> is  $< 3 \times 10^{-13} \text{ cm}^3 \text{ molec}^{-1} \text{ s}^{-1}$ , which leads to a tropospheric lifetime of more than 35 days ([OH] =  $1.1 \times 10^6 \text{ molec/cm}^3$ ) (Falbe-Hansen et al., 2000), over twenty times longer than DMS. A recent study (Berasategui et al., 2019) measured a rate constant of  $1.4 \pm (0.2) \times 10^{-13} \text{ cm}^3 \text{ molec}^{-1} \text{ s}^{-1}$  for the reaction of OH with MSAM, which results in a tropospheric lifetime of 75 days ([OH] =  $1.1 \times 10^6 \text{ molec/cm}^3$ ). As MSAM has a long lifetime with respect to reaction with OH, we must also consider its physical removal by deposition to the ocean surface. We therefore carried out experiments to determine the Henry's law constant for MSAM (details see Sect. S2) and found it to be in the range  $3.3 \times 10^4 \text{ M atm}^{-1}$ – $6.5 \times 10^5 \text{ M atm}^{-1}$ . DMSO<sub>2</sub> has a similarly large Henry's law constant  $> 5 \times 10^4 \text{ M atm}^{-1}$  (Lynch et al., 1994). The exchange flux between the gas and aqueous phase can be described phenomenologically to derive an estimate of the effective lifetimes (Schwartz, 1992; Yang et al., 2014). Because of the high Henry's law constant for both MSAM and DMSO<sub>2</sub>, to a good approximation their lifetime is dependent on the wind speed and the marine boundary layer height (details see Sect. S1). The lifetimes for a marine boundary layer height of  $750 \pm 250$  meters and wind speeds in the range from  $4 \text{ m s}^{-1}$  to  $14 \text{ m s}^{-1}$ , as encountered during the second leg in the Arabian Sea, is  $40 \pm 14$  hours and  $11 \pm 4$  hours respectively. During August the 12<sup>th</sup> and 13<sup>th</sup> airmasses from the Somalia upwelling most of the time traveled for 10 h up to a day before reaching the ship. On the 14<sup>th</sup> and 15<sup>th</sup> of August, airmasses from the Somalia upwelling were around 4 h old (determined from the HYSPLIT back trajectories). A common oceanic source and the similar lifetimes of DMSO<sub>2</sub> and MSAM help explain the observed good correlation of MSAM with DMSO<sub>2</sub> (see Fig. 4).

## 4.3 Chlorophyll exposure of HYSPLIT back trajectories

MSAM and DMSO<sub>2</sub> were close to the LOD during the first leg, despite the fact that DMS mixing ratios were even higher than during the second leg. This observation excludes a simple relationship between the emissions of DMS and DMSO<sub>2</sub>/MSAM. DMSO<sub>2</sub> is known to be an oxidation product of DMS and is therefore linked to marine biogenic activity (Barnes et al., 2006). We hypothesize that the newly detected trace gas MSAM is also linked to marine biogenic activity. This is based on the observation that MSAM displays the highest values when influenced mainly by remote marine air without recent contact with land, it correlates well with DMSO<sub>2</sub> (see Fig. 4 (c)) and is similar in chemical structure to DMS and DMSO<sub>2</sub>. A good indicator for marine biogenic activity is phytoplankton. Phytoplankton in the water can be detected from space via the *chlorophyll a* pigment used for photosynthesis. Satellite images of regional chlorophyll can be exploited to investigate emission areas of marine biogenic VOCs. In the following sections we will investigate, with the help of HYSPLIT back trajectories and *chlorophyll a* water content, where the source of MSAM and DMSO<sub>2</sub> is located.



### 4.3.1 *Chlorophyll a* water content

We used data from the satellite MODIS-aqua (Jackson et al., 2019). In Fig. 6 a-d) the *chlorophyll a* concentration averaged over 8 days is plotted for the time periods relevant for our measurements. During the first leg (Fig. 6 a, b) the ship entered the Arabian Sea region on the 19<sup>th</sup> of July and left it around the 23<sup>rd</sup> of July 2017. Figure 6 a) displays the average *chlorophyll a* distribution from the 12<sup>th</sup> until the 19<sup>th</sup> of July, since air masses reaching the ship from July 19<sup>th</sup> onwards will have traveled over *chlorophyll a* regions before the time of observation. For the second leg (Fig. 6 c,d) (12<sup>th</sup> of August till the 16<sup>th</sup> of August 2017) we used the average *chlorophyll a* content from the 5<sup>th</sup> of August till the 12<sup>th</sup> of August and from the 13<sup>th</sup> till the 20<sup>th</sup> of August. The highest *chlorophyll a* concentrations in the region are found off the Horn of Africa/Somalia coast, a strong upwelling region.

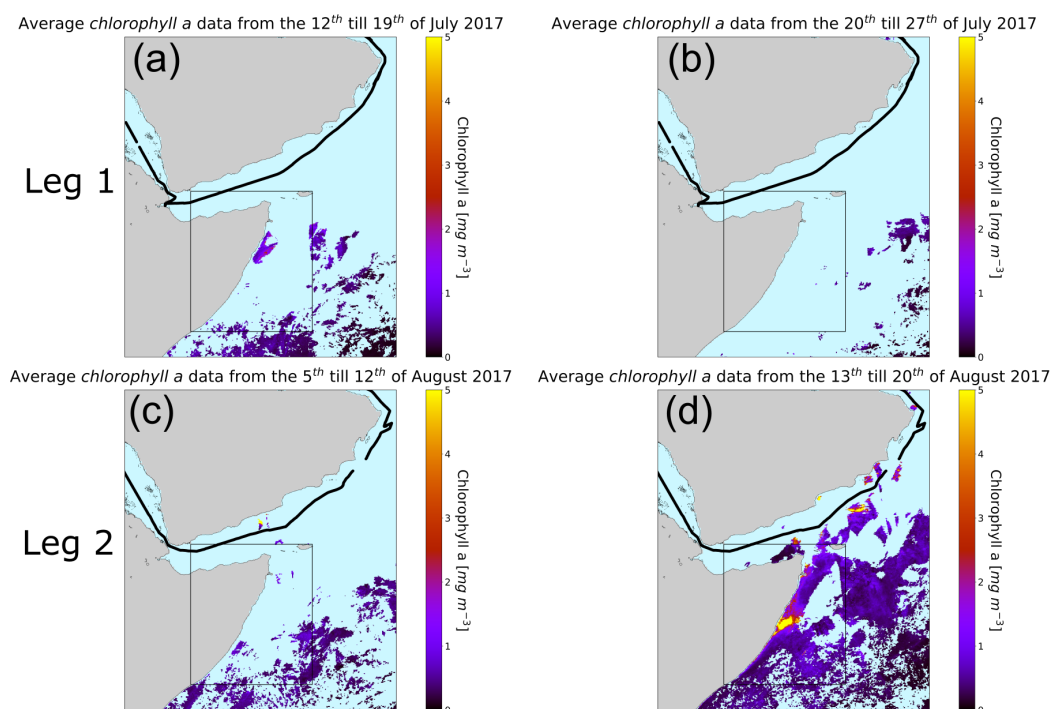


**Figure 6.** Eight day averaged *chlorophyll a* concentration in the Arabian Sea. The relevant time periods for the first leg (a,b) and for the second leg (c,d) are pictured here. Plot (a) represents the average *chlorophyll a* concentration from the 12<sup>th</sup> until the 19<sup>th</sup> of July, plot (b) from the 20<sup>th</sup> until the 27<sup>th</sup> of July, plot (c) from the 5<sup>th</sup> till the 12<sup>th</sup> of August and plot (d) from the 13<sup>th</sup> till the 20<sup>th</sup> of August. The black rectangle represents the region of the Somalia coast upwelling. The ship track is plotted in black. The light blue means no *chlorophyll a* content.





### 4.3.2 Back-trajectory-chlorophyll analysis

Air-masses arriving at the ship which have traveled over marine areas with high biological activity (meaning high phytoplankton content) likely contain higher levels of marine emissions. To investigate the provenance of air-masses sampled at the ship in relation to the chlorophyll distributions shown above, HYSPLIT back-trajectories were calculated (9 days back) for every full hour of the cruise. A weighting factor was applied to emphasize regions closer to the ship. In order to determine quantitatively to what extent the air sampled had passed over areas of high phytoplankton content (indexed with *chlorophyll a*), we summed up the *chlorophyll a* content detected by satellite in the water for each trajectory. Only time points when the trajectory was within the marine boundary layer, as calculated from the HYSPLIT model, were considered. The weighting factor ( $w$ ) is applied to this calculation by multiplying the *chlorophyll a* water content by:  $w = \frac{1}{1+p \cdot t}$ , where  $p$  is the weighting parameter and  $t$  is the number of hours before arrival at the ship's location. This was to account for the fact that marine emissions from phytoplankton closer to the ship will have a bigger impact on the measured mixing ratios as they will undergo less oxidation and dispersion. Several weighting factors were applied in order to determine the impact of the various parameters on the results. The weighting parameters  $p$  ranged from  $p = 0.02$  to  $p = 1$  and for exponential weighting factors in the form  $w_{exp} = p^t$ ,  $p$  was varied from  $p = 0.8$  to  $p = 0.99$  (details see Sect. S3). Varying these parameters did not affect the conclusions drawn.

The results of these calculations are displayed in Fig. 7. The graphs show the total chlorophyll exposure and the exposure of chlorophyll specifically from the region of the Somalia upwelling (see Fig. 6 the region in the black rectangle). In the first leg (Fig. 7 (a)), when both DMSO<sub>2</sub> and MSAM mixing ratios were low, air reaching the ship did not cross *chlorophyll a* rich waters in the previous 1 to 2 days. This is the case for the total exposure as well as for the exposure to chlorophyll in the Somalia upwelling region.

However, during the second leg (Fig. 7 (b)), when DMSO<sub>2</sub> and MSAM levels were high, the air measured had traveled over extensive *chlorophyll a* rich waters. In general, the exposure in the Somalia upwelling region always constituted the majority of the total exposure, except for one peak in the beginning (August 13<sup>th</sup> from 12:00 till 19:00) where chlorophyll patches closer to the ship constituted roughly half of the total chlorophyll exposure. From these calculations we can conclude that the occurrence of DMSO<sub>2</sub> and MSAM is related to marine emissions in the Somalia upwelling region. MSAM and DMSO<sub>2</sub> mixing ratios started to increase around midday of August 12<sup>th</sup> but the chlorophyll exposure only started to increase around 6:00 on August 13<sup>th</sup> (Fig. 7 (b)). The reason for this being trajectories arriving on August 12<sup>th</sup> had seen low *chlorophyll a* water content, as displayed in Fig. 6 (c), where no phytoplankton bloom was present in the Somalia upwelling region resulting in low chlorophyll exposure. This bloom developed afterward as seen in Fig. 6 (d) but might have started already on August 12<sup>th</sup> and escaped detection by MODIS-aqua. An inspection of daily data from MODIS-aqua revealed that parts of the Somalia upwelling were in a blind spot of the satellite on August 12<sup>th</sup>. The chlorophyll exposure sharply fell to zero at the beginning of the 15<sup>th</sup> of August, roughly 8 h before DMSO<sub>2</sub> and MSAM values start to decline as well (Fig. 7 (b)). In this case the calculated HYSPLIT back-trajectories no longer pass over the Somalia upwelling but cross Somalia before arriving at the ship. Our measurements thus indicate that we were impacted by the Somalian upwelling region for longer than calculated

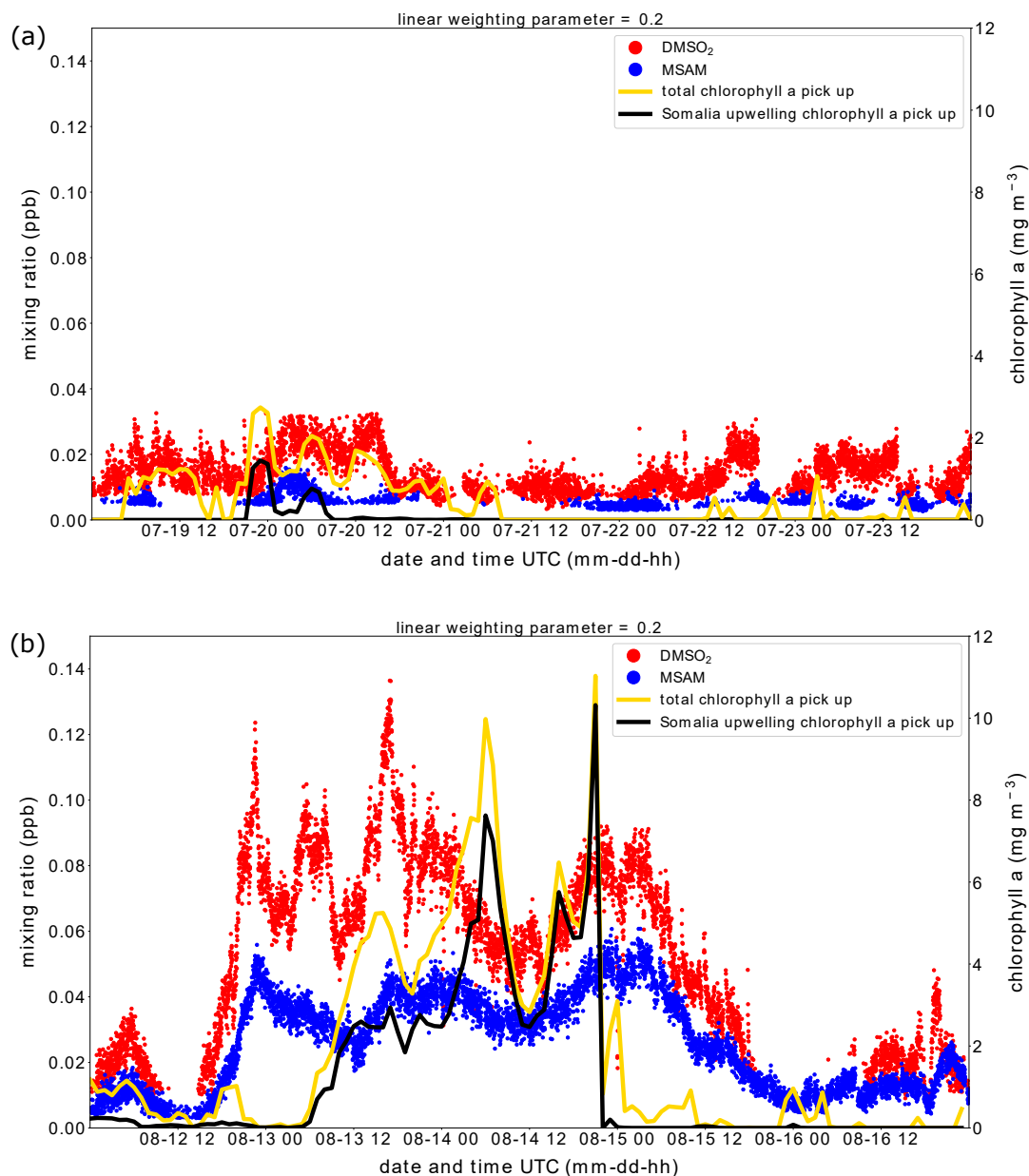


**Figure 7.** Weighted amount of *chlorophyll a* trajectories crossed over before arrival at the ship for leg 1 (a) and leg 2 (b). The total *chlorophyll a* exposure (yellow line) and the *chlorophyll a* exposure originating from the Somalia upwelling region (black line) is plotted. The corresponding y-axis for the *chlorophyll a* exposure for both graphs (a,b) is displayed on the right side. Measured ambient mixing ratios in ppb for DMSO<sub>2</sub> and MSAM are plotted in red and blue with the corresponding y-axis on the left side.



from the trajectories. This is not unexpected as meteorological data for this region are sparse, and the trajectories therefore correspondingly uncertain.

#### 4.4 DMSO<sub>2</sub>, DMSO, MSIA and MSA

We observed DMSO<sub>2</sub> mixing ratios during the second leg between 0.04 and 0.12 ppb, which is high compared to previous measurements of 0.2–11 ppb (Berresheim et al., 1998; D. Davis et al., 1998) made in Antarctica. As mentioned in the introduction, DMSO<sub>2</sub> is known to be formed from oxidation of DMS with OH, BrO or NO<sub>3</sub> (see Fig. 1). However, laboratory studies indicate that OH oxidation of DMS, via the intermediate DMSO, forms mainly methane sulfinic acid (MSIA) and not DMSO<sub>2</sub> (Barnes et al., 2006; Kukui et al., 2003; Hoffmann et al., 2016). BrO oxidation of DMSO generating DMSO<sub>2</sub> will be negligible for concentrations of 2 ppt for BrO, which have been proposed to be ubiquitous in the marine troposphere (Read et al., 2008; Platt and Hönninger, 2003), due to the slow reaction compared to the reaction with OH. NO<sub>3</sub> oxidation of DMSO was found to only yield DMSO<sub>2</sub> (Falbe-Hansen et al., 2000), but during the night, due to the lack of OH and BrO producing DMSO, DMSO<sub>2</sub> generation will be hindered.

With the data presented here it is not possible to decide which of the above mentioned mechanisms is responsible for the observed DMSO<sub>2</sub>. We did not detect DMSO, MSIA or methane sulfonic acid (MSA). DMSO is known to be an important intermediate in the oxidation of DMS with OH (Hoffmann et al., 2016). The reaction rate of DMSO with OH is 15 times faster than that of DMS with OH, making it a potentially important sink in the remote marine atmosphere (Barnes et al., 2006). A model study of the sulfur cycle in the global marine atmosphere suggested values of around 10 ppt for DMSO in the region of the Arabian Sea (Chen et al., 2018). This is below the limit of detection (LOD) of around 15 ppt for DMSO in our instrument and probably the reason why we do not observe it in this dataset. Measurements of DMSO made on Amsterdam Island ranged from 0.36 to 11.6 ppt (Sciare et al., 2000).

MSIA has a very high reaction rate of  $9 \times 10^{-11} \text{ cm}^3 \text{ molec}^{-1} \text{ s}^{-1}$  with OH radicals (Burkholder et al., 2015; Kukui et al., 2003; Hoffmann et al., 2016). In the model study mentioned above, this leads to concentrations over the Arabian Sea of around 2 ppt which again is below the LOD for MSIA with our instrument (around 20 ppt) (Chen et al., 2018).

MSA, on the other hand, is predicted to be around 20–40 ppt over the Arabian Sea (gas phase and aqueous phase combined), which is above its LOD, but almost all of it will be in the aqueous phase (Chen et al., 2018; Hoffmann et al., 2016). In the gas phase, the maximum MSA values reported to date are below 1 ppt, which is far too low to be measured with our setup (LOD around 15 ppt) (Eisele and Tanner, 1993; Chen et al., 2016; Berresheim, 2002).

#### 4.5 MSAM

We are not aware of a possible formation pathway for MSAM in the gas phase, therefore we consider it rather unlikely that it is formed via DMS gas phase oxidation. A microbial formation from DMS or DMS products in the water of the highly biological active upwelling region and subsequent emission into the atmosphere seems plausible (see Fig. 1). To our knowledge, no measurements of MSAM have been reported in the atmosphere so far and thus no information about the potential role it could play there is available. SO<sub>2</sub>, which oxidizes to sulfuric acid (H<sub>2</sub>SO<sub>4</sub>), is an oxidation product of MSAM (Gerasategui et al.,



2019).  $\text{H}_2\text{SO}_4$  is known to be a key contributor to new particle formation (Li et al., 2018; Kulmala et al., 2014; Almeida et al., 2013; Sipilä et al., 2010; Weber et al., 2001, 1996; Chen et al., 2016). However, due to the slow reaction of MSAM with OH, the contribution of MSAM to  $\text{SO}_2$  is negligible (Berasategui et al., 2019). Acid-base reactions (e.g.  $\text{H}_2\text{SO}_4$  with ammonia/amines) are very important in new particle formation (Chen and Finlayson-Pitts, 2017; Almeida et al., 2013). MSAM is an acid and therefore could participate in acid-base reactions, but since MSAM is only a weak acid ( $pK_a = 10.8$  (Junttila and Hormi, 2009)) its role as an acid in these reactions is probably limited.

Studies indicate, that the dominant driving force in new particle formation and growth are the hydrogen bonds formed between common atmospheric nucleation precursors (Xie et al., 2017; Cheng et al., 2017; Li et al., 2018). The newly found trace gas MSAM is very intriguing because it contains a sulfonamide group, which is a sulfonyl group connected to an amine group. The sulfonyl and the amine group both support hydrogen bonding, giving MSAM a high hydrogen-bonding capacity, potentially enabling nucleation.

Because of the comparable lifetimes of MSAM and DMS, we can estimate the relative emission of MSAM to DMS from the ratio of the mixing ratios of ( $[\text{MSAM}]/[\text{DMS}]$ ). We only included ratios observed in the afternoons of 14<sup>th</sup> and 15<sup>th</sup> of August, when the ship was in closest proximity to the Somalia upwelling. The afternoon was chosen to ensure that OH, the primary oxidant of DMS, was present. We derived ratios ranging from 0.1 to 0.27, meaning that emissions of MSAM over the Somalia upwelling can be almost a third of the DMS emissions. Therefore, MSAM could play an important role in particle formation and/or growth over and downwind of upwelling regions. To verify these possibilities, further experiments regarding particle growth and formation with MSAM need to be performed.

## 5 Conclusions

During the AQABA campaign we made the first measurements of MSAM in ambient air. Back-trajectories-chlorophyll analyses suggest that it is a marine biogenic emission from the highly productive upwelling region off Somalia. During the first leg of the AQABA campaign the ship encountered mostly biogenic emissions from sources located along the ship route when crossing the Arabian Sea. The enhanced DMS values observed there could be attributed to seasonally enhanced DMS fluxes and small local phytoplankton blooms visible from space along the Arabian Sea transect. No oxidation products or other organosulfur compounds were detected in substantial amounts from the local emissions. In contrast, during the second leg not only DMS but also  $\text{DMSO}_2$  and MSAM were measured.  $\text{DMSO}_2$ , like MSAM, was shown to originate from the Somalia upwelling region.  $\text{DMSO}_2$  mixing ratios of up to 0.12 ppb were measured during the second leg, which is quite substantial considering that previous studies indicate it to be a minor or negligible product in DMS gas phase oxidation. MSAM is a molecule which, to our knowledge, was never reported in the atmosphere. We detected it in concentrations up to 0.06 ppb during the second leg in the Arabian Sea. Emissions of MSAM over the Somalia upwelling can reach close to a third of the DMS emissions.

A marine emission containing a nitrogen atom is somewhat surprising since under most circumstances primary productivity in the ocean is nitrogen limited. The emission of a nitrogen containing compound may be related to the abundance of reactive nitrogen provided by the upwelling. Emissions of reactive nitrogen containing species have been previously measured from



upwelling (alkyl nitrates in equatorial upwelling (Chuck et al., 2002)). Due to its sulfonyl and amine group, MSAM has a high hydrogen-bonding capacity enabling hydrogen bonding to other atmospheric nucleation precursors. These hydrogen bonds are known to be a critical factor in particle growth and formation (Li et al., 2018; Xie et al., 2017; Cheng et al., 2017). Therefore MSAM could prove to be of importance for particle formation and/or growth over upwelling regions. The mechanisms in which gas phase precursors lead to new particle formation is an active research area in atmospheric chemistry because it is subject to large uncertainties (Li et al., 2018; Chen et al., 2016, 2018; Carslaw et al., 2013).

*Data availability.* Data will be made available via: <https://edmond.mpdl.mpg.de/imeji/>

*Author contributions.* AE and CS were responsible for VOC measurements and data. AE analysed the data and drafted the article. EP contributed laboratory experiments concerning Henry's law constant. MB and JC contributed to data interpretation. DW calculated the back trajectories. JL designed and realized the campaign. JW supervised the study. All authors contributed to manuscript writing and revision, read and approved the submitted version.

*Competing interests.* The authors declare that they have no conflict of interest.

*Acknowledgements.* We thankfully acknowledge the cooperation with the Cyprus Institute (CyI), the King Abdullah University of Science and Technology (KAUST) and the Kuwait Institute for Scientific Research (KISR). We thank Hays Ships Ltd, Captain Pavel Kirzner and the ship crew for their support on-board the Kommandor Iona. We would like to express our gratitude to the whole AQABA team, particularly Hartwig Harder for daily management of the campaign; and Marcel Dorf, Claus Koeppel, Thomas Klüpfel and Rolf Hofmann for logistical organization and help with preparation and setup. We are thankful to Jan Schuladen for the J-value measurements, Ulrike Weis for providing artificial seawater and Tom Jobson and Franziska Köllner for helpful discussions. The campaign was funded by the Max Planck Society.



## References

- Ajith Joseph, K., Jayaram, C., Nair, A., George, M. S., Balchand, A. N., and Pettersson, L. H.: Remote Sensing of Upwelling in the Arabian Sea and Adjacent Near-Coastal Regions, in: Remote sensing of the Asian Seas, edited by Barale, V. and Gade, M., vol. 92, pp. 467–483, Springer, Cham, Switzerland, [https://doi.org/10.1007/978-3-319-94067-0\\_26](https://doi.org/10.1007/978-3-319-94067-0_26), 2019.
- 5 Albu, M., Barnes, I., Becker, K. H., Patroescu-Klotz, I., Mocanu, R., and Benter, T.: Rate coefficients for the gas-phase reaction of OH radicals with dimethyl sulfide: temperature and O<sub>2</sub> partial pressure dependence, *Physical Chemistry Chemical Physics*, 8, 728–736, <https://doi.org/10.1039/B512536G>, <https://pubs.rsc.org/en/content/articlepdf/2006/cp/b512536g>, 2006.
- Almeida, J., Schobesberger, S., Kürten, A., Ortega, I. K., Kupiainen-Määttä, O., Praplan, A. P., Adamov, A., Amorim, A., Bianchi, F., Breitenlechner, M., David, A., Dommen, J., Donahue, N. M., Downard, A., Dunne, E., Duplissy, J., Ehrhart, S., Flagan, R. C., Franchin, A., Guida, R., Hakala, J., Hansel, A., Heinritzi, M., Henschel, H., Jokinen, T., Junninen, H., Kajos, M., Kangasluoma, J., Keskinen, H., Kupc, A., Kurtén, T., Kvashin, A. N., Laaksonen, A., Lehtipalo, K., Leiminger, M., Leppä, J., Loukonen, V., Makhmutov, V., Mathot, S., McGrath, M. J., Nieminen, T., Olenius, T., Onnela, A., Petäjä, T., Riccobono, F., Riipinen, I., Rissanen, M., Rondo, L., Ruuskanen, T., Santos, F. D., Sarnela, N., Schallhart, S., Schnitzhofer, R., Seinfeld, J. H., Simon, M., Sipilä, M., Stozhkov, Y., Stratmann, F., Tomé, A., Tröstl, J., Tsagko-georgas, G., Vaattovaara, P., Viisanen, Y., Virtanen, A., Vrtala, A., Wagner, P. E., Weingartner, E., Wex, H., Williamson, C., Wimmer, D.,
- 10 Ye, P., Yli-Juuti, T., Carslaw, K. S., Kulmala, M., Curtius, J., Baltensperger, U., Worsnop, D. R., Vehkamäki, H., and Kirkby, J.: Molecular understanding of sulphuric acid–amine particle nucleation in the atmosphere, *Nature*, 502, 359–363, <https://doi.org/10.1038/nature12663>, <https://www.nature.com/articles/nature12663.pdf>, 2013.
- Arnold, S. R., v. Spracklen, D., Gebhardt, S., Custer, T., Williams, J., Peeken, I., and Alvain, S.: Relationships between atmospheric organic compounds and air-mass exposure to marine biology, *Environmental Chemistry*, 7, 232, <https://doi.org/10.1071/EN09144>, 2010.
- 20 Ayers, G. P. and Gillett, R. W.: DMS and its oxidation products in the remote marine atmosphere: implications for climate and atmospheric chemistry, *Journal of Sea Research*, pp. 275–286, 2000.
- Barnes, I., Hjorth, J., and Mihalopoulos, N.: Dimethyl sulfide and dimethyl sulfoxide and their oxidation in the atmosphere, *Chemical reviews*, 106, 940–975, <https://doi.org/10.1021/cr020529>, 2006.
- Bentley, R. and Chasteen, T. G.: Environmental VOSCs—formation and degradation of dimethyl sulfide, methanethiol and related materials, *Chemosphere*, 55, 291–317, <https://doi.org/10.1016/j.chemosphere.2003.12.017>, 2004.
- 25 Berasategui, M., Amedro, D., Edtbauer, A., Williams, J., Lelieveld, J., and Crowley, J. N.: Kinetic and mechanistic study of the reaction between methane sulphonamide (CH<sub>3</sub>S(O)<sub>2</sub>NH<sub>2</sub>) and OH, in preparation, 2019.
- Berresheim, H.: Gas-aerosol relationships of H<sub>2</sub>SO<sub>4</sub>, MSA, and OH: Observations in the coastal marine boundary layer at Mace Head, Ireland, *Journal of Geophysical Research*, 107, 24, 191, <https://doi.org/10.1029/2000JD000229>, 2002.
- 30 Berresheim, H., Huey, J. W., Thorn, R. P., Eisele, F. L., Tanner, D. J., and Jefferson, A.: Measurements of dimethyl sulfide, dimethyl sulfoxide, dimethyl sulfone, and aerosol ions at Palmer Station, Antarctica, *Journal of Geophysical Research*, 1998, 1629–1637, 1998.
- Bonsang, B., Gros, V., Peeken, I., Yassaa, N., Bluhm, K., Zoellner, E., Sarda-Estève, R., and Williams, J.: Isoprene emission from phytoplankton monocultures: the relationship with chlorophyll-a, cell volume and carbon content, *Environmental Chemistry*, 7, 554, <https://doi.org/10.1071/EN09156>, 2010.
- 35 Bourtsoukidis, E., Ernle, L., Crowley, J. N., Lelieveld, J., Paris, J.-D., Pozzer, A., Walter, D., and Williams, J.: Non-methane hydrocarbon (C<sub>2</sub>–C<sub>8</sub>) sources and sinks around the Arabian Peninsula, *Atmospheric Chemistry and Physics*, 19, 7209–7232, <https://doi.org/10.5194/acp-19-7209-2019>, <https://www.atmos-chem-phys.net/19/7209/2019/acp-19-7209-2019.pdf>, 2019.





- Breider, T. J., Chipperfield, M. P., d. Richards, N. A., Carslaw, K. S., Mann, G. W., and v. Spracklen, D.: Impact of BrO on dimethylsulfide in the remote marine boundary layer, *Geophysical Research Letters*, 37, <https://doi.org/10.1029/2009GL040868>, <https://agupubs.onlinelibrary.wiley.com/doi/full/10.1029/2009GL040868>, 2010.
- Bruyn, W. J. D., Shorter, J. A., Davidovits, P., Worsnop, D. R., Zahniser, M. S., and Kolb, C. E.: Uptake of gas phase sulfur species  
 5 methanesulfonic acid, dimethylsulfoxide, and dimethyl sulfone by aqueous surfaces, *Journal of Geophysical Research: Atmospheres*, 99, 16 927–16 932, <https://doi.org/10.1029/94JD00684>, <https://agupubs.onlinelibrary.wiley.com/doi/full/10.1029/94JD00684>, 1994.
- Burkholder, J. B., Sander, S. P., Abbatt, J., Barker, J. R., Huie, R. E., Kolb, C. E., Kurylo, M. J., Orkin, V. L., Wilmouth, D. M., and Wine, P. H.: Chemical Kinetics and Photochemical Data for Use in Atmospheric Studies, Evaluation Number 18, JPL Publication 15-10, Jet Propulsion Laboratory, Pasadena, <https://doi.org/10.13140/RG.2.1.2504.2806>, 2015.
- 10 Carslaw, K. S., Lee, L. A., Reddington, C. L., Pringle, K. J., Rap, A., Forster, P. M., Mann, G. W., v. Spracklen, D., Woodhouse, M. T., Regayre, L. A., and Pierce, J. R.: Large contribution of natural aerosols to uncertainty in indirect forcing, *Nature*, 503, 67, <https://doi.org/10.1038/nature12674>, <https://www.nature.com/articles/nature12674.pdf>, 2013.
- Chen, H. and Finlayson-Pitts, B. J.: New Particle Formation from Methanesulfonic Acid and Amines/Ammonia as a Function of Temperature, *Environmental science & technology*, 51, 243–252, <https://doi.org/10.1021/acs.est.6b04173>, 2017.
- 15 Chen, H., Varner, M. E., Gerber, R. B., and Finlayson-Pitts, B. J.: Reactions of Methanesulfonic Acid with Amines and Ammonia as a Source of New Particles in Air, *The journal of physical chemistry. B*, 120, 1526–1536, <https://doi.org/10.1021/acs.jpcc.5b07433>, 2016.
- Chen, Q., Sherwen, T., Evans, M., and Alexander, B.: DMS oxidation and sulfur aerosol formation in the marine troposphere: a focus on reactive halogen and multiphase chemistry, *Atmospheric Chemistry and Physics*, 18, 13 617–13 637, <https://doi.org/10.5194/acp-18-13617-2018>, 2018.
- 20 Cheng, S., Tang, S., Tsona, N. T., and Du, L.: The Influence of the Position of the Double Bond and Ring Size on the Stability of Hydrogen Bonded Complexes, *Scientific reports*, 7, 11 310, <https://doi.org/10.1038/s41598-017-11921-7>, <https://www.nature.com/articles/s41598-017-11921-7.pdf>, 2017.
- Chesnavich, W. J., Su, T., and Bowers, M. T.: Collisions in a noncentral field: A variational and trajectory investigation of ion–dipole capture, *The Journal of Chemical Physics*, 72, 2641–2655, <https://doi.org/10.1063/1.439409>, 1980.
- 25 Chuck, A. L., Turner, S. M., and Liss, P. S.: Direct Evidence for a Marine Source of C1 and C2 Alkyl Nitrates, *Science*, 297, 1151–1154, <https://doi.org/10.1126/science.1073896>, <https://science.sciencemag.org/content/sci/297/5584/1151.full.pdf>, 2002.
- Colomb, A., Yassaa, N., Williams, J., Peeken, I., and Lochte, K.: Screening volatile organic compounds (VOCs) emissions from five marine phytoplankton species by head space gas chromatography/mass spectrometry (HS-GC/MS), *Journal of environmental monitoring : JEM*, 10, 325–330, <https://doi.org/10.1039/b715312k>, 2008.
- 30 D. Davis, G. Chen, P. Kasibhatla, A. Jefferson, D. Tanner, F. Eisele, D. Lenschow, W. Neff, and H. Berresheim: DMS oxidation in the Antarctic marine boundary layer: Comparison of model simulations and held observations of DMS, DMSO, DMSO<sub>2</sub>,<br>H<sub>2</sub>SO<sub>4</sub>(g), MSA(g), and MSA(p), *Journal of Geophysical Research*, 1998, 1657–1678, 1998.
- deCastro, M., Sousa, M. C., Santos, F., Dias, J. M., and Gómez-Gesteira, M.: How will Somali coastal upwelling evolve under future warming scenarios?, *Scientific reports*, 6, 30 137, <https://doi.org/10.1038/srep30137>, 2016.
- 35 Derstroff, B., Hüser, I., Bourtsoukidis, E., Crowley, J. N., Fischer, H., Gromov, S., Harder, H., Janssen, R. H. H., Kesselmeier, J., Lelieveld, J., Mallik, C., Martinez, M., Novelli, A., Parchatka, U., Phillips, G. J., Sander, R., Sauvage, C., Schuladen, J., Stönnner, C., Tomsche, L., and Williams, J.: Volatile organic compounds (VOCs) in photochemically aged air from the eastern and western Mediterranean, *Atmospheric Chemistry and Physics*, 17, 9547–9566, <https://doi.org/10.5194/acp-17-9547-2017>, 2017.



- Draxler, R. R. and Hess, G.: An Overview of the HYSPLIT \_ 4 Modelling System for Trajectories , Dispersion , and Deposition, <https://pdfs.semanticscholar.org/b534/55cef2115b8b26cb1deb44d3dccb1b5e0d16.pdf>, 1998.
- Eisele, F. L. and Tanner, D. J.: Measurement of the gas phase concentration of H<sub>2</sub>SO<sub>4</sub> and methane sulfonic acid and estimates of H<sub>2</sub>SO<sub>4</sub> production and loss in the atmosphere, *Journal of Geophysical Research*, 98, 9001–9010, <https://doi.org/10.1029/93JD00031>, 1993.
- 5 Falbe-Hansen, H., Sørensen, S., Jensen, N. R., Pedersen, T., and Hjorth, J.: Atmospheric gas-phase reactions of dimethylsulphoxide and dimethylsulphone with OH and NO<sub>3</sub> radicals, Cl atoms and ozone, *Atmospheric Environment*, 34, 1543–1551, [https://doi.org/10.1016/S1352-2310\(99\)00407-0](https://doi.org/10.1016/S1352-2310(99)00407-0), 2000.
- Ge, X., Wexler, A. S., and Clegg, S. L.: Atmospheric amines – Part I. A review, *Atmospheric Environment*, 45, 524–546, <https://doi.org/10.1016/j.atmosenv.2010.10.012>, <http://www.sciencedirect.com/science/article/pii/S1352231010008745>, 2011.
- 10 Graus, M., Müller, M., and Hansel, A.: High resolution PTR-TOF: quantification and formula confirmation of VOC in real time, *Journal of the American Society for Mass Spectrometry*, 21, 1037–1044, <https://doi.org/10.1016/j.jasms.2010.02.006>, 2010.
- Hoffmann, E. H., Tilgner, A., Schrödner, R., Bräuer, P., Wolke, R., and Herrmann, H.: An advanced modeling study on the impacts and atmospheric implications of multiphase dimethyl sulfide chemistry, *Proceedings of the National Academy of Sciences of the United States of America*, 113, 11 776–11 781, <https://doi.org/10.1073/pnas.1606320113>, 2016.
- 15 Jackson, T., Chuprin, A., Sathyendranath, S., Grant, M., Zühlke, M., Dingle, J., Storm, T., Boettcher, M., and Fomferra, N.: Ocean Colour Climate Change Initiative: version 4.0, [ftp://ftp.rsg.pml.ac.uk/occci-v4.0/geographic/netcdf/8day/chlor\\_a/2017/](ftp://ftp.rsg.pml.ac.uk/occci-v4.0/geographic/netcdf/8day/chlor_a/2017/), 2019.
- Jordan, A., Haidacher, S., Hanel, G., Hartungen, E., Märk, L., Seehauser, H., Schottkowsky, R., Sulzer, P., and Märk, T. D.: A high resolution and high sensitivity proton-transfer-reaction time-of-flight mass spectrometer (PTR-TOF-MS), *International Journal of Mass Spectrometry*, 286, 122–128, <https://doi.org/10.1016/j.ijms.2009.07.005>, 2009.
- 20 Junttila, M. H. and Hormi, O. O. E.: Methanesulfonamide: a cosolvent and a general acid catalyst in sharpless asymmetric dihydroxylations, *The Journal of organic chemistry*, 74, 3038–3047, <https://doi.org/10.1021/jo8026998>, 2009.
- Khan, M., Gillespie, S., Razis, B., Xiao, P., Davies-Coleman, M. T., Percival, C. J., Derwent, R. G., Dyke, J. M., Ghosh, M. V., Lee, E., and Shallcross, D. E.: A modelling study of the atmospheric chemistry of DMS using the global model, STOCHEM-CRI, *Atmospheric Environment*, 127, 69–79, <https://doi.org/10.1016/j.atmosenv.2015.12.028>, 2016.
- 25 Kiene, R. P., Linn, L. J., and Bruton, J. A.: New and important roles for DMSP in marine microbial communities, *Journal of Sea Research*, 43, 209–224, [https://doi.org/10.1016/S1385-1101\(00\)00023-X](https://doi.org/10.1016/S1385-1101(00)00023-X), 2000.
- Kloster, S., Feichter, J., Maier-Reimer, E., Six, K. D., Stier, P., and Wetzol, P.: DMS cycle in the marine ocean-atmosphere system – a global model study, *Biogeosciences*, 3, 29–51, [https://pure.mpg.de/pubman/item/item\\_994660\\_3/component/file\\_994659/Biogeosci\\_3-29.pdf](https://pure.mpg.de/pubman/item/item_994660_3/component/file_994659/Biogeosci_3-29.pdf), 2006.
- 30 Kämpf, J. and Chapman, P.: *Upwelling Systems of the World*, Springer International Publishing, Cham, <https://doi.org/10.1007/978-3-319-42524-5>, 2016.
- Kukui, A., Borissenko, D., Laverdet, G., and Le Bras, G.: Gas-Phase Reactions of OH Radicals with Dimethyl Sulfoxide and Methane Sulfinic Acid Using Turbulent Flow Reactor and Chemical Ionization Mass Spectrometry, *The Journal of Physical Chemistry A*, 107, 5732–5742, <https://doi.org/10.1021/jp0276911>, 2003.
- 35 Kulmala, M., Petäjä, T., Ehn, M., Thornton, J., Sipilä, M., Worsnop, D. R., and Kerminen, V.-M.: Chemistry of atmospheric nucleation: on the recent advances on precursor characterization and atmospheric cluster composition in connection with atmospheric new particle formation, *Annual review of physical chemistry*, 65, 21–37, <https://doi.org/10.1146/annurev-physchem-040412-110014>, 2014.



- Lai, S. C., Williams, J., Arnold, S. R., Atlas, E. L., Gebhardt, S., and Hoffmann, T.: Iodine containing species in the remote marine boundary layer: A link to oceanic phytoplankton, *Geophysical Research Letters*, 38, n/a–n/a, <https://doi.org/10.1029/2011GL049035>, 2011.
- Lana, A., Bell, T. G., Simó, R., Vallina, S. M., Ballabrera-Poy, J., Kettle, A. J., Dachs, J., Bopp, L., Saltzman, E. S., Stefels, J., Johnson, J. E., and Liss, P. S.: An updated climatology of surface dimethylsulfide concentrations and emission fluxes in the global ocean, *Global Biogeochemical Cycles*, 25, n/a–n/a, <https://doi.org/10.1029/2010GB003850>, 2011.
- Li, H., Zhang, X., Zhong, J., Liu, L., Zhang, H., Chen, F., Li, Z., Li, Q., and Ge, M.: The role of hydroxymethanesulfonic acid in the initial stage of new particle formation, *Atmospheric Environment*, 189, 244–251, <https://doi.org/10.1016/j.atmosenv.2018.07.003>, <http://www.sciencedirect.com/science/article/pii/S1352231018304424>, 2018.
- Lindinger, W., Hansel, A., and Jordan, A.: On-line monitoring of volatile organic compounds at pptv levels by means of proton-transfer-reaction mass spectrometry (PTR-MS) medical applications, food control and environmental research, *International Journal of Mass Spectrometry and Ion Processes*, 173, 191–241, [https://doi.org/10.1016/S0168-1176\(97\)00281-4](https://doi.org/10.1016/S0168-1176(97)00281-4), 1998.
- Liss, P. S., Marandino, C. A., Dahl, E. E., Helmig, D., Hints, E. J., Hughes, C., Johnson, M. T., Moore, R. M., Plane, J. M. C., Quack, B., Singh, H. B., Stefels, J., von Glasow, R., and Williams, J.: Short-Lived Trace Gases in the Surface Ocean and the Atmosphere, in: *Ocean-Atmosphere Interactions of Gases and Particles*, edited by Liss, P. and Johnson, M. T., Springer Earth System Sciences, pp. 1–54, Springer-Verlag GmbH, [Erscheinungsort nicht ermittelbar], [https://doi.org/10.1007/978-3-642-25643-1\\_1](https://doi.org/10.1007/978-3-642-25643-1_1), [https://doi.org/10.1007/978-3-642-25643-1\\_1](https://doi.org/10.1007/978-3-642-25643-1_1), 2014.
- Mardyukov, A. and Schreiner, P. R.: Atmospherically Relevant Radicals Derived from the Oxidation of Dimethyl Sulfide, *Accounts of chemical research*, 51, 475–483, <https://doi.org/10.1021/acs.accounts.7b00536>, 2018.
- Pfannerstill, E. Y., Wang, N., Edtbauer, A., Bourtsoukidis, E., Crowley, J. N., Dienhart, D., Eger, P. G., Ernle, L., Fischer, H., Hottmann, B., Paris, J.-D., Stöner, C., Tadic, I., Walter, D., Lelieveld, J., and Williams, J.: Shipborne measurements of total OH reactivity around the Arabian Peninsula and its role in ozone chemistry, *Atmospheric Chemistry and Physics Discussions*, pp. 1–38, <https://doi.org/10.5194/acp-2019-416>, <https://www.atmos-chem-phys-discuss.net/acp-2019-416/acp-2019-416.pdf>, 2019.
- Platt, U. and Hönninger, G.: The role of halogen species in the troposphere, *Chemosphere*, 52, 325–338, [https://doi.org/10.1016/S0045-6535\(03\)00216-9](https://doi.org/10.1016/S0045-6535(03)00216-9), <http://www.sciencedirect.com/science/article/pii/S0045653503002169>, 2003.
- Quinn, P. K. and Bates, T. S.: The case against climate regulation via oceanic phytoplankton sulphur emissions, *Nature*, 480, 51–56, <https://doi.org/10.1038/nature10580>, 2011.
- Read, K. A., Mahajan, A. S., Carpenter, L. J., Evans, M. J., Faria, B. V. E., Heard, D. E., Hopkins, J. R., Lee, J. D., Moller, S. J., Lewis, A. C., Mendes, L., McQuaid, J. B., Oetjen, H., Saiz-Lopez, A., Pilling, M. J., and Plane, J. M. C.: Extensive halogen-mediated ozone destruction over the tropical Atlantic Ocean, *Nature*, 453, 1232–1235, <https://doi.org/10.1038/nature07035>, <https://www.nature.com/articles/nature07035.pdf>, 2008.
- Schwartz, S. E.: Factors Governing Dry Deposition of Gases to Surface-Water, in: *PRECIPITATION SCAVENGING AND ATMOSPHERE-SURFACE EXCHANGE, VOLS 1-3*, edited by Schwartz, S. E. and SLINN, W. G., pp. 789–801, HEMISPHERE PUBL CORP, NEW YORK, 1992.
- Sciare, J., Kanakidou, M., and Mihalopoulos, N.: Diurnal and seasonal variation of atmospheric dimethylsulfoxide at Amsterdam Island in the southern Indian Ocean, *JOURNAL OF GEOPHYSICAL RESEARCH*, pp. 17 257–17 265, 2000.
- Sipilä, M., Berndt, T., Petäjä, T., Brus, D., Vanhanen, J., Stratmann, F., Patokoski, J., Mauldin, R. L., Hyvärinen, A.-P., Lihavainen, H., and Kulmala, M.: The Role of Sulfuric Acid in Atmospheric Nucleation, *Science*, 327, 1243–1246, <https://doi.org/10.1126/science.1180315>, <https://science.sciencemag.org/content/sci/327/5970/1243.full.pdf>, 2010.



- Su, T. and Chesnavich, W. J.: Parametrization of the ion–polar molecule collision rate constant by trajectory calculations, *The Journal of Chemical Physics*, 76, 5183–5185, <https://doi.org/10.1063/1.442828>, 1982.
- Veres, P. R., Faber, P., Drewnick, F., Lelieveld, J., and Williams, J.: Anthropogenic sources of VOC in a football stadium: Assessing human emissions in the atmosphere, *Atmospheric Environment*, 77, 1052–1059, <https://doi.org/10.1016/j.atmosenv.2013.05.076>, 2013.
- 5 Vila-Costa, M., Simó, R., Harada, H., Gasol, J. M., Slezak, D., and Kiene, R. P.: Dimethylsulfoniopropionate uptake by marine phytoplankton, *Science (New York, N.Y.)*, 314, 652–654, <https://doi.org/10.1126/science.1131043>, 2006.
- Voss, M., Bange, H. W., Dippner, J. W., Middelburg, J. J., Montoya, J. P., and Ward, B.: The marine nitrogen cycle: recent discoveries, uncertainties and the potential relevance of climate change, *Philosophical transactions of the Royal Society of London. Series B, Biological sciences*, 368, 20130 121, <https://doi.org/10.1098/rstb.2013.0121>, 2013.
- 10 Warneke, C. and de Gouw, J. A.: Organic trace gas composition of the marine boundary layer over the northwest Indian Ocean in April 2000, *Atmospheric Environment*, 35, 5923–5933, [https://doi.org/10.1016/S1352-2310\(01\)00384-3](https://doi.org/10.1016/S1352-2310(01)00384-3), 2001.
- Webb, A. L., van Leeuwe, M. A., den Os, D., Meredith, M. P., J Venables, H., and Stefels, J.: Extreme spikes in DMS flux double estimates of biogenic sulfur export from the Antarctic coastal zone to the atmosphere, *Scientific reports*, 9, 2233, <https://doi.org/10.1038/s41598-019-38714-4>, 2019.
- 15 Weber, R. J., MARTI, J. J., McMURRY, P. H., Eisele, F. L., Tanner, D. J., and Jefferson, A.: MEASURED ATMOSPHERIC NEW PARTICLE FORMATION RATES: IMPLICATIONS FOR NUCLEATION MECHANISMS, *Chemical Engineering Communications*, 151, 53–64, <https://doi.org/10.1080/00986449608936541>, 1996.
- Weber, R. J., Chen, G., Davis, D. D., Mauldin, R. L., Tanner, D. J., Eisele, F. L., Clarke, A. D., Thornton, D. C., and Bandy, A. R.: Measurements of enhanced H<sub>2</sub>SO<sub>4</sub> and 3–4 nm particles near a frontal cloud during the First Aerosol Characterization Experiment (ACE 1), *Journal of Geophysical Research: Atmospheres*, 106, 24 107–24 117, <https://doi.org/10.1029/2000JD000109>, <https://agupubs.onlinelibrary.wiley.com/doi/full/10.1029/2000JD000109>, 2001.
- 20 Williams, J., Custer, T., Riede, H., Sander, R., Jöckel, P., Hoor, P., Pozzer, A., Wong-Zehnpfennig, S., Hosaynali Beygi, Z., Fischer, H., Gros, V., Colomb, A., Bonsang, B., Yassaa, N., Peeken, I., Atlas, E. L., Waluda, C. M., van Aardenne, J. A., and Lelieveld, J.: Assessing the effect of marine isoprene and ship emissions on ozone, using modelling and measurements from the South Atlantic Ocean, *Environmental Chemistry*, 7, 171, <https://doi.org/10.1071/EN09154>, 2010.
- 25 Xie, H.-B., Elm, J., Halonen, R., Myllys, N., Kurtén, T., Kulmala, M., and Vehkamäki, H.: Atmospheric Fate of Monoethanolamine: Enhancing New Particle Formation of Sulfuric Acid as an Important Removal Process, *Environmental science & technology*, 51, 8422–8431, <https://doi.org/10.1021/acs.est.7b02294>, 2017.
- Yang, M., Beale, R., Liss, P., Johnson, M., Blomquist, B., and Nightingale, P.: Air–sea fluxes of oxygenated volatile organic compounds across the Atlantic Ocean, *Atmospheric Chemistry and Physics*, 14, 7499–7517, <https://doi.org/10.5194/acp-14-7499-2014>, <https://www.atmos-chem-phys.net/14/7499/2014/acp-14-7499-2014.pdf>, 2014.
- 30 Yassaa, N., Peeken, I., Zöllner, E., Bluhm, K., Arnold, S., Spracklen, D., and Williams, J.: Evidence for marine production of monoterpenes, *Environmental Chemistry*, 5, 391, <https://doi.org/10.1071/EN08047>, 2008.
- Zavarsky, A., Booge, D., Fiehn, A., Krüger, K., Atlas, E., and Marandino, C.: The Influence of Air–Sea Fluxes on Atmospheric Aerosols During the Summer Monsoon Over the Tropical Indian Ocean, *Geophysical Research Letters*, 45, 418–426, <https://doi.org/10.1002/2017GL076410>, 2018.